Optimizations of Multi-hop Cooperative Molecular Communication in Cylindrical Anomalous-Diffusive Channel

Xuancheng Jin[1], Zhen Cheng[1], Zhian Ye[1], and Weihua Gong[1]
[1] School of Computer Science and Technology, Zhejiang University of Technology
Hangzhou, 310023, China
[e-mail: xuanchengjin@zjut.edu.cn, chengzhen@zjut.edu.cn, 202203151328@zjut.edu.cn, whgong@zjut.edu.cn]
*Corresponding author: Zhen Cheng

Received November 13, 2023; revised March 3, 2024; accepted April 3, 2024; published April 30, 2024

Abstract

In this paper, the optimizations of multi-hop cooperative molecular communication (CMC) system in cylindrical anomalous-diffusive channel in three-dimensional enviroment are investigated. First, we derive the performance of bit error probability (BEP) of CMC system under decode-and-forward relay strategy. Then for achieving minimum average BEP, the optimization variables are detection thresholds at cooperative nodes and destination node, and the corresponding optimization problem is formulated. Furthermore, we use conjugate gradient (CG) algorithm to solve this optimization problem to search optimal detection thresholds. The numerical results show the optimal detection thresholds can be obtained by CG algorithm, which has good convergence behaviors with fewer iterations to achieve minimized average BEP compared with gradient decent algorithm and Bisection method which are used in molecular communication.

Keywords: Cooperative molecular communication, Cylindrical anomalous-diffusive channel, Optimizations, Conjugate gradient algorithm

This work was supported in part by National Natural Science Foundation of China (Grant Nos. 62271446); in part by Zhejiang Provincial Natural Science Foundation of China (Grant Nos. LY23F020021).

http://doi.org/10.3837/tiis.2024.04.014 **ISSN : 1976-7277**

1. Introduction

The field of molecular communication (MC) [1-2] attracts more attentions of many researchers because of its application prospects in biological environments and industrial fields [3-5]. Recently, more studies have been focused on MC with diffusion in an unbounded fluid environment [6-7].

However, MC in an unbounded environment has some limitations in the practical applications due to its channel characteristics, such as in the blood vessel of human body [8]. Then MC in bounded environment has attracted a lot of attentions of many researchers. The authors [9-10] analytically derived the concentration Green's function (CGF) of MC system in biological cylindrical channel. Based on the Poiseuille flow and the Robin boundary condition, the authors [11] utilized a Markovian-based channel model for MC system to deduce the probability density function. In 2022, Dhok et al. [12] evaluated the performance of probability error of a cooperative molecular communication (CMC) system in cylindrical environment by using a fusion center.

Usually, the molecules propagate in the channel which follows the conventional Brownian motion. However, the scenario of the anomalous diffusion is more extensive comparing with conventional Brownian motion. In 2017, Mai et al. [13] proposed an algorithm for optimizing the network throughput in MC system with anomalous diffusion. In 2019, Trinh et al. [14] derived the first passage time of the molecules by using timing modulation. In 2020, Chouhan et al. [15] calculated the bit error probability (BEP) based on deriving the expression of first passage time density of MC system. In 2021, Trinh et al. [16] derived the observed molecules and the closed-form expressions of the bit error rate. In 2022, the formulation of the first hitting time density of anomalous-diffusive MC system was deduced in [17]. The authors in [18] considered the anomalous diffusion and derived the expression of the CGF of an underlay cognitive MC system.

As so far, some traditional algorithms are used to obtain optimal decision threshold in order to achieve minimum BEP of MC system. Tavakkoli et al. [19] minimized the BEP of two-hop MC system by using bisection algorithm to obtain optimal detection threshold. Chouhan et al. [20] implemented gradient descent (GD) optimization for finding the solutions of the optimization problem which are the values of optimization variables including optimal decision threshold of MC system. Cheng et al. implemented particle swarm optimization algorithm [21] and adaptive genetic algorithm [22] to solve different optimization problems in order to achieve minimum BEP of MC system.

However, the multi-hop CMC system in cylindrical anomalous-diffusive channel in three-dimensional (3D) environment has not been studied. On one hand, because of multiple relay nodes in the CMC system, there are multiple detection thresholds needed to be computed by using the maximum a posteriori (MAP) probability detection method with multiple times. However, all the detection thresholds at cooperative nodes and destination node can be obtained simultaneously by using the optimization algorithm. On the other hand, the detection thresholds are optimized by minimizing the average BEP of the CMC system. Therefore, the optimized detection thresholds can improve the reliability of communication of the CMC system. In order to obtain minimum BEP of this system, how to optimize the detection thresholds at cooperative nodes and destination node is a challenge study. But the existing traditional algorithms needs more iterations. It is important to develop more efficient offline optimization techniques. In this paper, we use the conjugate gradient (CG) algorithm to solve the optimization problem. The main contributions of our paper are concluded as follows:

(1) The decode-and-forward (DF) relaying strategy is implemented at cooperative nodes for

the multi-hop CMC system. Then the formulation of average BEP is derived.

(2) We set up an optimization problem for achieving minimum average BEP with optimization variables which are detection thresholds at cooperative nodes and destination node. Then CG algorithm is adopted to solve this optimization problem for searching the optimal detection thresholds.

(3) The numerical results have revealed that CG algorithm is more efficient in finding the optimal detection thresholds at cooperative nodes and the destination node with fewer iterations compared with GD algorithm and Bisection method.

The rest of our paper is organized as follows. Section 2 presents the CMC system model in 3D environment. In Section 3, the detection thresholds are optimized by CG algorithm. In Section 4, the performances of this CMC system with optimized detection thresholds are evaluated. Section 5 summarizes the paper.

2. The Multi-hop CMC System

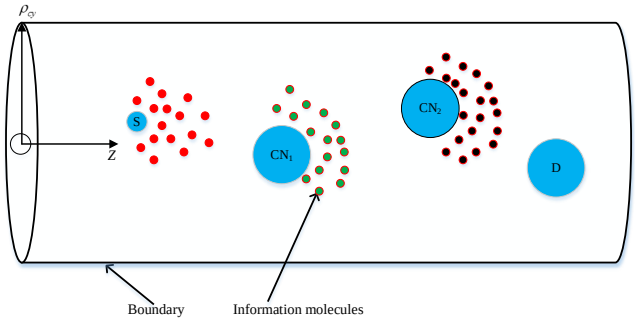

Fig. 1. The multi-hop CMC system.

The system model of multi-hop CMC in cylindrical channel with anomalous diffusion and drift in 3D enviroment is shown in **Fig. 1**. This cylindrical channel with the radius ρ_{cy} is a semi-infinite cylinder with boundary. This system is composed of one source node S, K cooperative nodes CN_1, CN_2, …, CN_K and one destination node D, which have fixed locations denoted by (ρ_S, ϕ_S, z_S), $(\rho_{CN_1}, \phi_{CN_1}, z_{CN_1})$, $(\rho_{CN_2}, \phi_{CN_2}, z_{CN_2})$, … , $(\rho_{CN_K}, \phi_{CN_K}, z_{CN_K})$, (ρ_D, ϕ_D, z_D), respectively. Here, (ρ, ϕ, z) describes the radial, azimuthal and axial coordinates of each node, respectively. In addition, we have $0 \le \rho \le \rho_{cy}$, $0 \le \phi < 2\pi$. In the axial direction, it extends from origin to infinity, then the range of z is $0 \le z < \infty$.

We assume that the transmission time is time-slotted. Each time slot duration is T_s. The modulation method of ON/OFF keying [23] is adopted. The node S and K cooperative nodes instantaneously release molecules at the beginning of each time slot for transmitting bit 1, while releasing no molecules represents the transmission of bit 0. We also suppose that source node S, K cooperative nodes and node D can keep perfect synchronization in time [24-25].

After the transmission process starts, the DF relaying strategy is adopted at each relay node. Different types of molecules are used in each hop. When time slot j begins, the source node S releases molecules with type A_1 for transmitting bit 1. For the DF relaying, when time slot j ends, the cooperative node CN_1 receives the transmitted bit, which is forwarded to its adjacent node CN_2 when next time slot begins. Each node CN_k (k=1, 2, ... , K) can detect type A_k molecules from node CN_{k-1} at the end of time slot (j+k-1). Then it releases A_{k+1} molecule types

to forward the decoded bit to node CN_{k+1}. CN_0 and CN_{K+1} represent node S node D, respectively. The cooperative nodes and node D are the passive spherical receivers with the radius r_{CN_k} (k=1, 2, ... , K) and r_D , respectively. In each time slot, they can count the number of molecules to make the decision that the received bit is 1 or 0 by comparing with the detection thresholds.

After node S and cooperative nodes release molecules, these molecules diffuse in cylindrical anomalous channel. This process can be modeled based on the type of diffusion phenomenon. $D_\alpha(t)$ represents the instantaneous diffusion coefficient which is computed by [26]

$$D_\alpha(t) = \alpha D_p t^{\alpha-1}, \tag{1}$$

where D_p represents the diffusion coefficient of molecules. $\alpha \in [0,2]$ is the diffusion exponent which is defined by the normal diffusion with α =1, sub-diffusion with $\alpha \in [0,1)$ and super-diffusion with $\alpha \in (1,2]$.

The CGF under the Robin's boundary condition shows the concentration of molecules at node S at time t with location (ρ_S, ϕ_S, z_S) under given initial time t_0, which is denoted by $C_S(t;t_0)$ [9]

$$C_S(t;t_0) = \frac{\exp\left(-\dfrac{(z-z_S-v(t-t_0))^2}{4(t-t_0)^\alpha D_p} - \xi(t-t_0)\right)}{\sqrt{4\pi(t-t_0)^\alpha D_p}} \times \left(\sum_{n=0}^{\infty}\sum_{m=1}^{\infty} Q_{nm}\cos(n(\phi-\phi_S))J_n(\lambda_{nm}\rho)\times\exp(-D_p\lambda_{nm}^2(t-t_0)^\alpha)\delta(t-t_0)\right), \tag{2}$$

where z_S is the coordinate value along z axis. v is the drift velocity. ξ is the degradation constant. ρ_S and ρ_{cy} are the radii of node S and the cylindrical channel, respectively. t_0 is the initial time instant. $Q_{nm} = \dfrac{L_n J_n(\lambda_{nm}\rho_S)}{N_{nm}}$, $N_{nm} = \dfrac{\rho_{cy}^2}{2}\left(J_n^2(\lambda_{nm}\rho_{cy}) - J_{n-1}(\lambda_{nm}\rho_{cy})J_{n+1}(\lambda_{nm}\rho_{cy})\right)$.

J_n and λ_{nm} are the n-th order Bessel function of the first kind and the m-th eigenvalues, respectively. J_{n-1} and J_{n+1} are defined as J_n. n and m are integers. L_n and $\delta(t)$ are given as follows:

$$L_n = \begin{cases} \dfrac{1}{\pi}, & n \geq 1, \\ \dfrac{1}{2\pi}, & n = 0, \end{cases} \tag{3}$$

$$\delta(t-t_0) = \begin{cases} 1, & t \geq t_0, \\ 0, & t < t_0. \end{cases} \tag{4}$$

The probability of the case that one released molecule is observed at node CN_1 at time t is obtained by [9]

$$p_{(S,CN_1)}(t;t_0) = \iiint_{V_{CN_1}} C_S(t;t_0)\rho \, d\rho d\phi dz. \tag{5}$$

where V_{CN_1} is the volume of node CN_1 which a spherical region. Then (5) is approximated as $p_{(\mathrm{S},\mathrm{CN}_1)}(t;t_0)=V_{\mathrm{CN}_1}C_{\mathrm{S}}(t;t_0)$. When t_0 represents the l-th time slot in which one molecule emitted by node S, the probability of the case that this one molecule is observed in time slot j by node CN_1 is given by

$$p_{(\mathrm{S},\mathrm{CN}_1)}^{lj}=V_{\mathrm{CN}_1}C_{\mathrm{S}}((j-l)T_s;t_0). \tag{6}$$

3. Derivation of average BEP of the CMC system

$N_{\mathrm{S}}[l]$ and x_{S}^{l} $(1\le l\le j)$ are used to denote the quantity of released molecules and the transmitted bit by node S in time slot l, respectively. In time slot j, considering the reception at node CN_1, $N_{(\mathrm{S},\mathrm{CN}_1)}[j]$ is defined as the quantity of received molecules. Then we have

$$N_{(\mathrm{S},\mathrm{CN}_1)}[j]=\sum_{l=1}^{j}N_{\mathrm{S}}[l]x_{\mathrm{S}}^{l}p_{(\mathrm{S},\mathrm{CN}_1)}^{lj}+N_{(\mathrm{S},\mathrm{CN}_1)}^{\mathrm{Noise}}, \tag{7}$$

where $N_{(\mathrm{S},\mathrm{CN}_1)}^{\mathrm{Noise}}$ is the noise generated for this link. It is modelled as a Normal distribution $\mathcal{N}\left(0,(\sigma_{(\mathrm{S},\mathrm{CN}_1)}^{\mathrm{Noise}})^2\right)$, which has mean 0 and variance $(\sigma_{(\mathrm{S},\mathrm{CN}_1)}^{\mathrm{Noise}})^2$ [25].

When $N_{\mathrm{S}}[l]$ is large enough, according to the central limit theorem [25], $N_{(\mathrm{S},\mathrm{CN}_1)}[j]$ is modelled as Gaussian approximation. Therefore, we have

$$N_{(\mathrm{S},\mathrm{CN}_1)}[j]\sim\mathcal{N}\left(\mu_{(\mathrm{S},\mathrm{CN}_1)}[j],\sigma_{(\mathrm{S},\mathrm{CN}_1)}^{2}[j]\right), \tag{8}$$

where $\mu_{(\mathrm{S},\mathrm{CN}_1)}[j]$ is the mean and $\sigma_{(\mathrm{S},\mathrm{CN}_1)}^{2}[j]$ is the variance of $N_{(\mathrm{S},\mathrm{CN}_1)}[j]$, which are obtained as follows:

$$\mu_{(\mathrm{S},\mathrm{CN}_1)}[j]=\sum_{l=1}^{j}\pi_1N_{\mathrm{S}}[k]p_{(\mathrm{S},\mathrm{CN}_1)}^{lj}, \tag{9}$$

$$\sigma_{(\mathrm{S},\mathrm{CN}_1)}^{2}[j]=\sum_{l=1}^{j}\left[\pi_1N_{\mathrm{S}}[l]p_{(\mathrm{S},\mathrm{CN}_1)}^{lj}\left(1-p_{(\mathrm{S},\mathrm{CN}_1)}^{lj}\right)+(N_{\mathrm{S}}[l])^2\pi_1\pi_0(p_{(\mathrm{S},\mathrm{CN}_1)}^{kj})^2\right]+(\sigma_{(\mathrm{S},\mathrm{CN}_1)}^{\mathrm{Noise}})^2, \tag{10}$$

where π_1 and π_0 are the transmission probabilities of 1 and 0 by node S when each time slot begins, respectively. We have $\Pr(x_{\mathrm{S}}[l]=1)=\pi_1=0.5$ and $\Pr(x_{\mathrm{S}}[l]=0)=\pi_0=0.5$.

H_0 and H_1 indicate the cases that when time slot j begins, node S transmits bits 0 and 1, respectively. Then the corresponding Normal distributions under H_0 and H_1 are formulated by

$$\begin{aligned}H_0&:N_{(\mathrm{S},\mathrm{CN}_1)}[j]\sim\mathcal{N}\left(\mu_{(\mathrm{S},\mathrm{CN}_1)}^{0}[j],(\sigma_{(\mathrm{S},\mathrm{CN}_1)}^{0}[j])^2\right),\\ H_1&:N_{(\mathrm{S},\mathrm{CN}_1)}[j]\sim\mathcal{N}\left(\mu_{(\mathrm{S},\mathrm{CN}_1)}^{1}[j],(\sigma_{(\mathrm{S},\mathrm{CN}_1)}^{1}[j])^2\right),\end{aligned} \tag{11}$$

where $\mu_{(\mathrm{S},\mathrm{CN}_1)}^{w}[j]$ (w=0, 1) is the mean and $(\sigma_{(\mathrm{S},\mathrm{CN}_1)}^{w}[j])^2$ (w=0, 1) is the variance of $N_{(\mathrm{S},\mathrm{CN}_1)}[j]$ under H_w, respectively. According to (9) and (10), $\mu_{(\mathrm{S},\mathrm{CN}_1)}^{w}[j]$ and $(\sigma_{(\mathrm{S},\mathrm{CN}_1)}^{w}[j])^2$ (w=0, 1) can be computed by

$$\mu^0_{(\mathrm{S},\mathrm{CN}_1)}[j]=\sum_{l=1}^{j-1}\pi_1 N_{\mathrm{S}}[l]p^{l(j-1)}_{(\mathrm{S},\mathrm{CN}_1)},$$
$$(\sigma^0_{(\mathrm{S},\mathrm{CN}_1)}[j])^2=\sum_{l=1}^{j-1}\left[\pi_1 N_{\mathrm{S}}[l]p^{lj}_{(\mathrm{S},\mathrm{CN}_1)}\left(1-p^{lj}_{(\mathrm{S},\mathrm{CN}_1)}\right)+(N_{\mathrm{S}}[l])^2\pi_1\pi_0(p^{lj}_{(\mathrm{S},\mathrm{CN}_1)})^2\right]+(\sigma^{\mathrm{Noise}}_{(\mathrm{S},\mathrm{CN}_1)})^2, \quad (12)$$
$$\mu^1_{(\mathrm{S},\mathrm{CN}_1)}[j]=N_{\mathrm{S}}[j]p^{jj}_{(\mathrm{S},\mathrm{CN}_1)}+\mu^0_{(\mathrm{S},\mathrm{CN}_1)}[j],$$
$$(\sigma^1_{(\mathrm{S},\mathrm{CN}_1)}[j])^2=N_{\mathrm{S}}[j]p^{jj}_{(\mathrm{S},\mathrm{CN}_1)}\left(1-p^{jj}_{(\mathrm{S},\mathrm{CN}_1)}\right)+(\sigma^0_{(\mathrm{S},\mathrm{CN}_1)}[j])^2.$$

The detection threshold at node CN_1 is η_{CN_1}. Then when each time slot ends, the detection rule at node CN_1 is written as

$$\hat{x}_{\mathrm{CN}_1}[j]=\begin{cases}1, \ if \ N_{(\mathrm{S},\mathrm{CN}_1)}[j]\geq\eta_{\mathrm{CN}_1},\\ 0, \ if \ N_{(\mathrm{S},\mathrm{CN}_1)}[j]<\eta_{\mathrm{CN}_1},\end{cases} \quad (13)$$

where $\hat{x}^j_{\mathrm{CN}_1}$ is denoted by the bit decoded by node CN_1 when time slot j ends. When $x^j_{\mathrm{S}}\neq\hat{x}^j_{\mathrm{CN}_1}$, an error occurs in this time slot. $\Pr(\hat{x}^j_{\mathrm{CN}_1}=0\,|\,x^j_{\mathrm{S}}=1)$ and $\Pr(\hat{x}^j_{\mathrm{CN}_1}=1\,|\,x^j_{\mathrm{S}}=0)$ represent the error probabilities of bits transmission of 1 and 0, respectively. Then we have

$$\begin{aligned}\Pr(\hat{x}^j_{\mathrm{CN}_1}=0\,|\,x^j_{\mathrm{S}}=1)&=\Pr(N_{(\mathrm{S},\mathrm{CN}_1)}[j]<\eta_{\mathrm{CN}_1}\,|\,x^j_{\mathrm{S}}=1)\\&=Q\left(\frac{\eta_{\mathrm{CN}_1}-\mu^0_{(\mathrm{S},\mathrm{CN}_1)}[j]}{\sigma^0_{(\mathrm{S},\mathrm{CN}_1)}[j]}\right),\end{aligned} \quad (14)$$

$$\begin{aligned}\Pr(\hat{x}^j_{\mathrm{CN}_1}=1\,|\,x^j_{\mathrm{S}}=0)&=\Pr(N_{(\mathrm{S},\mathrm{CN}_1)}[j]\geq\eta_{\mathrm{CN}_1}\,|\,x^j_{\mathrm{S}}=0)\\&=Q\left(\frac{\eta_{\mathrm{CN}_1}-\mu^1_{(\mathrm{S},\mathrm{CN}_1)}[j]}{\sigma^1_{(\mathrm{S},\mathrm{CN}_1)}[j]}\right),\end{aligned} \quad (15)$$

where the function $Q(x)$ is denoted by $Q(x)=\frac{1}{\sqrt{2\pi}}\int_x^\infty e^{-\frac{u^2}{2}}du$. Based on formulas (14) and (15), $Pe_{(\mathrm{S},\mathrm{CN}_1)}[j]$ which represents the BEP of one bit transmission in time slot j is written as

$$Pe_{(\mathrm{S},\mathrm{CN}_1)}[j]=\pi_1\Pr(\hat{x}^j_{\mathrm{CN}_1}=0\,|\,x^j_{\mathrm{S}}=1)+\pi_0\Pr(\hat{x}^j_{\mathrm{CN}_1}=1\,|\,x^j_{\mathrm{S}}=0). \quad (16)$$

Considering the link $\mathrm{CN}_k\rightarrow\mathrm{CN}_{k+1}$ in the (j+k)-th time slot, $N_{(\mathrm{CN}_k,\mathrm{CN}_{k+1})}[j+k]$ is the number of received molecules by CN_{k+1}. The binary hypothesis testing problem based on $N_{(\mathrm{CN}_k,\mathrm{CN}_{k+1})}[j+k]$ is established at node CN_{k+1} as follows:

$$\begin{aligned}H_0&: N_{(\mathrm{CN}_k,\mathrm{CN}_{k+1})}[j+k]\sim\mathcal{N}\left(\mu^0_{(\mathrm{CN}_k,\mathrm{CN}_{k+1})}[j],(\sigma^0_{(\mathrm{CN}_k,\mathrm{CN}_{k+1})}[j])^2\right),\\H_1&: N_{(\mathrm{CN}_k,\mathrm{CN}_{k+1})}[j+k]\sim\mathcal{N}\left(\mu^1_{(\mathrm{CN}_k,\mathrm{CN}_{k+1})}[j],(\sigma^1_{(\mathrm{CN}_k,\mathrm{CN}_{k+1})}[j])^2\right),\end{aligned} \quad (17)$$

where $\mu^w_{(\mathrm{CN}_k,\mathrm{CN}_{k+1})}[j]$ (w=0, 1) is the mean and $(\sigma^w_{(\mathrm{CN}_k,\mathrm{CN}_{k+1})}[j])^2$ (w=0, 1) is the variance of $N_{(\mathrm{CN}_k,\mathrm{CN}_{k+1})}[j+k]$ under H_w, respectively.

Let $x^{j+k}_{\mathrm{CN}_k}=0$ and $x^{j+k}_{\mathrm{CN}_k}=1$ represent the bits transmission of 0 and 1 by CN_k at the time

slot (j+k), respectively. $\hat{x}_{\mathrm{CN}_{k+1}}^{j+k}$ is 1 and 0 which are decoded by node CN_{k+1} when time slot (j+k) ends, respectively. Thus the corresponding error probabilities for the link $\mathrm{CN}_k \to \mathrm{CN}_{k+1}$ are defined as $\Pr(\hat{x}_{\mathrm{CN}_{k+1}}^{j+k}=1|x_{\mathrm{CN}_k}^{j+k}=0)$ and $\Pr(\hat{x}_{\mathrm{CN}_{k+1}}^{j+k}=0|x_{\mathrm{CN}_k}^{j+k}=1)$, respectively, which are computed according to (17) as follows:

$$\Pr(\hat{x}_{\mathrm{CN}_{k+1}}^{j+k}=1|x_{\mathrm{CN}_k}^{j+k}=0)=\Pr(N_{(\mathrm{CN}_k,\mathrm{CN}_{k+1})}[j+k]\ge\eta_{\mathrm{CN}_{k+1}}\mid x_{\mathrm{CN}_k}^{j+k}=0), \tag{18}$$

$$\Pr(\hat{x}_{\mathrm{CN}_{k+1}}^{j+k}=0|x_{\mathrm{CN}_k}^{j+k}=1)=\Pr(N_{(\mathrm{CN}_k,\mathrm{CN}_{k+1})}[j+k]<\eta_{\mathrm{CN}_{k+1}}\mid x_{\mathrm{CN}_k}^{j+k}=1), \tag{19}$$

where $\eta_{\mathrm{CN}_{k+1}}$ is detection threshold at node CN_{k+1}.

After node CN_{k+1} decodes the received bit, it forwards $\hat{x}_{\mathrm{CN}_{k+1}}^{j+k}$ to the next relay node CN_{k+2}. The transmitted bit by CN_{k+2} at the (j+k+1)-th time slot is $\hat{x}_{\mathrm{CN}_{k+1}}^{j+k+1}$. Assume the BEP of bit 0 or 1 transmission in time slot j from S to CN_k are $Pe_{(\mathrm{S},\mathrm{CN}_k)}^{0}[j]$ and $Pe_{(\mathrm{S},\mathrm{CN}_k)}^{1}[j]$, respectively. Then considering the link $\mathrm{S}\to\mathrm{CN}_{k+1}$, the BEP of one bit transmission in time slot j are computed by

$$\begin{aligned}Pe_{(\mathrm{S},\mathrm{CN}_{k+1})}^{0}[j]&=Pe_{(\mathrm{S},\mathrm{CN}_k)}^{0}[j]\times\Pr[\hat{x}_{\mathrm{CN}_{k+1}}^{j+k}=1\mid x_{\mathrm{CN}_k}^{j+k}=1]\\&\quad+(1-Pe_{(\mathrm{S},\mathrm{CN}_k)}^{0}[j])\times\Pr[\hat{x}_{\mathrm{CN}_{k+1}}^{j+k}=1\mid x_{\mathrm{CN}_k}^{j+k}=0],\end{aligned} \tag{20}$$

$$\begin{aligned}Pe_{(\mathrm{S},\mathrm{CN}_{k+1})}^{1}[j]&=Pe_{(\mathrm{S},\mathrm{CN}_k)}^{1}[j]\times\Pr[\hat{x}_{\mathrm{CN}_{k+1}}^{j+k}=0\mid x_{\mathrm{CN}_k}^{j+k}=0]\\&\quad+(1-Pe_{(\mathrm{S},\mathrm{CN}_k)}^{1}[j])\times\Pr[\hat{x}_{\mathrm{CN}_{k+1}}^{j+k}=0\mid x_{\mathrm{CN}_k}^{j+k}=1].\end{aligned} \tag{21}$$

When considering the multi-hop CMC system with k=K in (20) and (21), the BEP of one bit in the j-th time slot from node S denoted by $Pe_{(\mathrm{S},\mathrm{D})}[j]$ is computed by

$$Pe_{(\mathrm{S},\mathrm{D})}[j]=\pi_1 Pe_{(\mathrm{S},\mathrm{CN}_{K+1})}^{1}[j]+\pi_0 Pe_{(\mathrm{S},\mathrm{CN}_{K+1})}^{0}[j]. \tag{22}$$

4. Optimization of detection thresholds of multi-hop CMC system

The optimization problem of detection thresholds of the multi-hop CMC system in cylindrical channel is expressed as follows:

$$\min_{\eta_{\mathrm{CN}_1},\,\eta_{\mathrm{CN}_2},\ldots,\eta_{\mathrm{CN}_K},\eta_{\mathrm{D}}} Pe_{(\mathrm{S},\mathrm{D})}[j], \tag{23}$$

where $\eta_{\mathrm{CN}_1},\eta_{\mathrm{CN}_2},\ldots,\eta_{\mathrm{CN}_K}$ are the detection thresholds of nodes CN_1, CN_2, … , CN_K, respectively. η_{D} is the detection threshold at destination node D.

η_u is a vector of detection thresholds at the u-th iteration which is represented by $\eta_u=[\eta_{\mathrm{CN}_1}^{u},\eta_{\mathrm{CN}_2}^{u},\ldots,\eta_{\mathrm{CN}_K}^{u},\eta_{\mathrm{D}}^{u}]$. $\nabla Pe_{(\mathrm{S},\mathrm{D})}[j](\eta_u)$ is the gradient of $Pe_{(\mathrm{S},\mathrm{D})}[j]$ with η_u which is computed by

$$\nabla Pe_{(\mathrm{S},\mathrm{D})}[j](\eta_u)=\left[\frac{\partial Pe_{(\mathrm{S},\mathrm{D})}[j](\eta_u)}{\partial\eta_{\mathrm{CN}_1}},\frac{\partial Pe_{(\mathrm{S},\mathrm{D})}[j](\eta_u)}{\partial\eta_{\mathrm{CN}_2}},\ldots,\frac{\partial Pe_{(\mathrm{S},\mathrm{D})}[j](\eta_u)}{\partial\eta_{\mathrm{CN}_K}},\frac{\partial Pe_{(\mathrm{S},\mathrm{D})}[j](\eta_u)}{\partial\eta_{\mathrm{D}}}\right], \tag{24}$$

where $\frac{\partial Pe_{(\mathrm{S},\mathrm{D})}[j](\eta_u)}{\partial\eta_{\mathrm{CN}_1}},\frac{\partial Pe_{(\mathrm{S},\mathrm{D})}[j](\eta_u)}{\partial\eta_{\mathrm{CN}_2}},\ldots,\frac{\partial Pe_{(\mathrm{S},\mathrm{D})}[j](\eta_u)}{\partial\eta_{\mathrm{CN}_K}},\frac{\partial Pe_{(\mathrm{S},\mathrm{D})}[j](\eta_u)}{\partial\eta_{\mathrm{D}}}$ are the first

derivative of $Pe_{(\mathrm{S,D})}[j](\eta_u)$ with respect to $\eta_{\mathrm{CN}_1}, \eta_{\mathrm{CN}_2}, ..., \eta_{\mathrm{CN}_K}$, η_{D}, respectively. The CG algorithm is described as follows:

Algorithm 1. CG Algorithm for Optimizing Detection Thresholds in CMC System

Input: The maximum number of iterations is N=50. ε=0.0001 is the accuracy. Randomly set a starting point $\eta_0 = [\eta^0_{\mathrm{CN}_1}, \eta^0_{\mathrm{CN}_2}, ..., \eta^0_{\mathrm{CN}_K}, \eta^0_{\mathrm{D}}]$ which is composed of the initial value of detection thresholds at nodes CN_1, CN_2, … , CN_K and node D.

Output: The vector of optimal detection thresholds $\eta^* = [\eta^*_{\mathrm{CN}_1}, \eta^*_{\mathrm{CN}_2}, ..., \eta^*_{\mathrm{CN}_K}, \eta^*_{\mathrm{D}}]$.

for u = 0 to N do
  if u %K == 0
    Update decent direction: $\Delta(\eta_{u+1}) = -\nabla Pe_{(\mathrm{S,D})}[j](\eta_u)$.
  else
    $$\beta_{u+1} == \frac{(\nabla Pe_{(\mathrm{S,D})}[j](\eta_u))^T \nabla Pe_{(\mathrm{S,D})}[j](\eta_u)}{(\nabla Pe_{(\mathrm{S,D})}[j](\eta_{u-1}))^T \nabla Pe_{(\mathrm{S,D})}[j](\eta_{u-1})}.$$
    Update decent direction: $\Delta(\eta_{u+1}) = -\nabla Pe_{(\mathrm{S,D})}[j](\eta_u) + \beta_{u+1}\Delta(\eta_u)$.
  end if
  Choose step size γ_u for line search.
  Update $\eta_{u+1} = \eta_u + \gamma_u \Delta(\eta_{u+1})$, calculate $Pe_{(\mathrm{S,D})}[j](\eta_{u+1})$.
  Until $\left\| Pe_{(\mathrm{S,D})}[j](\eta_{u+1}) - Pe_{(\mathrm{S,D})}[j](\eta_u) \right\| \le \varepsilon$. Then output the vector which is composed of optimal detection thresholds $\eta^* = [\eta^*_{\mathrm{CN}_1}, \eta^*_{\mathrm{CN}_2}, ..., \eta^*_{\mathrm{CN}_K}, \eta^*_{\mathrm{D}}]$.
end for

It is noted that when $\left\| \nabla Pe_{(\mathrm{S,D})}[j](\eta_0) \right\| > \lambda (\lambda = 10^{-6})$ and the corresponding $Pe_{(\mathrm{S,D})}[j](\eta_0)$ at η_0 is smaller than 0.5, this algorithm can converge fast, and it performs exceptionally well. Then we can get optimized results of detection thresholds at cooperative nodes and destination node. When $\left\| \nabla Pe_{(\mathrm{S,D})}[j](\eta_0) \right\| \le \lambda$ and the corresponding $Pe_{(\mathrm{S,D})}[j](\eta_0)$ at η_0 is equal to 0.5, this algorithm is difficult to achieve convergence. Under such a case, this algorithm will face challenges. In order to solve this problem, we search for a better $\eta_0^{'}$ at the neighborhood of η_0 which can satisfy the condition that $\left\| \nabla Pe_{(\mathrm{S,D})}[j](\eta_0) \right\| > \lambda$. Then η_0 is updated as $\eta_0 = \eta_0^{'}$.

5. Numerical results

The numerical results are shown in this section and the default numerical parameters are given in **Table 1**.

Table 1. The numerical parameters

Parameter	Value	Parameter	Value
r_{CN_k}, r_D	2μm	D_p	1×10^{-10} m^2/s [18]
(ρ_S, ϕ_S, z_S)	(0,0,0)	v	65μm/s [18]
$(\rho_{CN_1}, \phi_{CN_1}, z_{CN_1})$	(2μm,0,5μm)	ξ	9s^{-1} [12]
$(\rho_{CN_2}, \phi_{CN_2}, z_{CN_2})$	(2μm,0,10μm)	ρ_{cy}	5μm [12]
(ρ_D, ϕ_D, z_D)	(2μm,0,15μm)	T_s	500ms
α	[0,2]	N	3×10^4

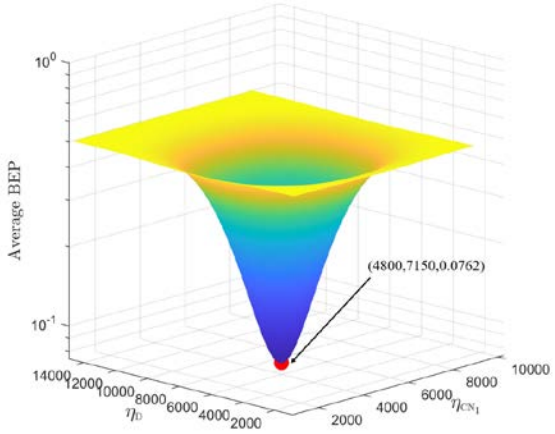

Fig. 2. The average BEP vs η_{CN_1} and η_D.

η_{CN_1} and η_D are the thresholds at node CN_1 and node D, respectively. **Fig. 2** shows the average BEP is changing with η_{CN_1} and η_D when there is one cooperation node CN_1. When η_{CN_1} takes the same value, the average BEP decreases first and then increases with the increasing value of η_D. The change trend under fixed value of η_D is the same as that under fixed value of η_{CN_1}. We can see that it is a convex problem when two detection thresholds with η_{CN_1} and η_D are optimized. Therefore, CG algorithm can be adopted to solve this optimization problem efficiently. The value of the lowest point with red dots is represented by (4800,7150, 0.0762), which means that the optimized results are η_{CN_1}=4800, η_D=7150 and the corresponding average BEP is 0.0762.

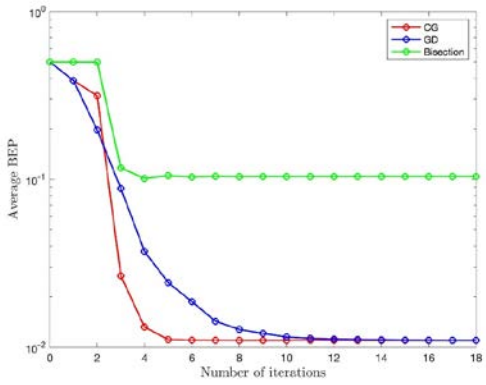

Fig. 3. The comparison results of convergence with CG, GD and Bisection algorithms.

In **Fig. 3**, we give the convergence analysis of CG, GD and Bisection algorithms. Under these three algorithms, when the number of iterations is increasing, the performances of average BEP are both decreasing. Finally, they can achieve convergence. We can see that CG algorithm converges fastest than GD algorithm and Bisection algorithm. We can see that for the same parameter setting, the number of iterations of CG algorithm, GD algorithm and Bisection algorithm are 5, 11 and 7, respectively. Therefore, we use CG algorithm to solve this optimization problem with fewer iterations and obtain optimal detection thresholds and minimum average BEP.

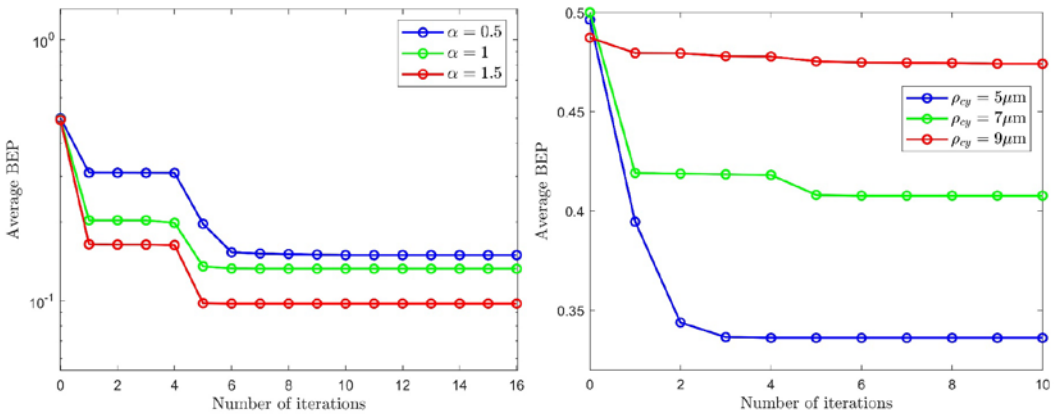

(a) (b)

Fig. 4. Convergence analysis under different values of (a) α ; (b) ρ_{cy} .

When α and ρ_{cy} take different values, the convergence results are shown in **Fig. 4(a)** and **Fig. 4(b)**, respectively. Here α is the diffusion exponent which has corresponding ranges. The CG algorithm has good convergence which shows that the average BEP can converge with fewer iterations. In **Fig. 4(a)**, when α = 0.5 and α =1.5, the corresponding number of iterations are 6 and 5, respectively. In **Fig. 4(b)**, when ρ_{cy} = 5μm and ρ_{cy} = 7μm, the average BEP achieves convergence within 3 iterations and 5 iterations, respectively. Second, when the values of α are smaller and the values of ρ_{cy} are larger, the average BEP are both larger.

This result is explained by the facts: on one hand, smaller values of α results in slower diffusion. On the other hand, larger values of ρ_{cy} means the same number of molecules can diffuse in much larger space. These two cases both lead to a decrease of the number of molecules received by cooperative nodes CN_1, CN_2 and node D, finally there is a decrease in BEP for each link.

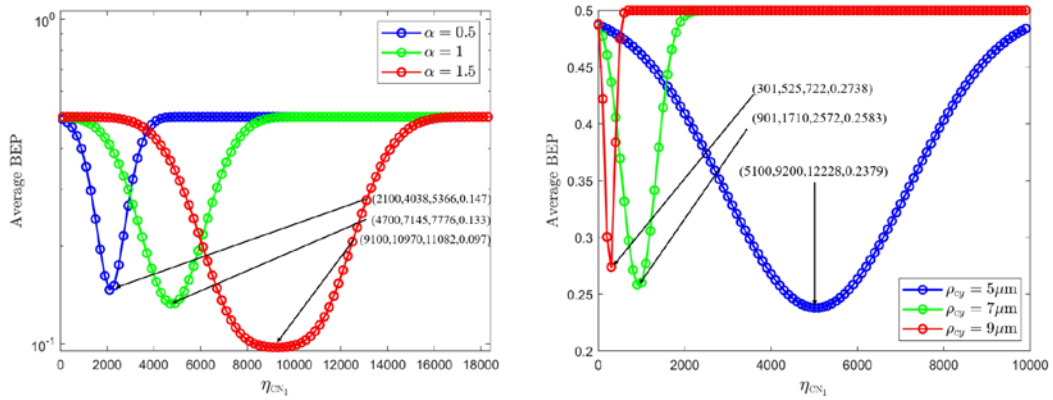

Fig. 5. The average BEP vs η_{CN_1} under different values of (a) α ; (b) ρ_{cy} .

The average BEP is changing with η_{CN_1} under different values of α and ρ_{cy} in **Fig. 5**. Different ranges in **Fig. 5(a)** including $\alpha < 1$, $\alpha = 1$ and $\alpha > 1$ represent sub-diffusion, normal diffusion and super-diffusion, respectively. We can see that when α is increasing, the average BEP is found to decrease. This is explained as follows: larger value of α will accelerate the diffusion of molecules. Then the number of molecules arriving at nodes CN_1, CN_2 and node D will increase. Finally, this reduces the average BEP. In addition, the optimal thresholds at CN_1, CN_2 and node D are given at the lowest point with minimum value of average BEP. When α =1.5, η_{CN_1} =9100, η_{CN_2} =10970, η_D =11082 and the corresponding average BEP is 0.097. In **Fig. 5(b)**, ρ_{cy} ={5μm, 7μm, 9μm}. The performance of average BEP is decreasing with η_{CN_1} . When η_{CN_1} achieves some value, the average BEP achieves its minimum value and then increase. Moreover, the number of received molecules is larger when ρ_{cy} takes smaller value, and the corresponding detection thresholds are also larger to obtain minimum value of average BEP. For the case ρ_{cy} =5μm, η_{CN_1} =5100, η_{CN_2} =9200, and η_D =12228, the average BEP is larger than those under the cases ρ_{cy} =7μm and ρ_{cy} =9μm.

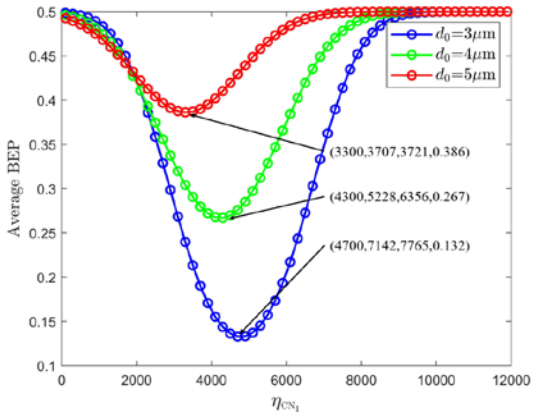

Fig. 6. The average BEP vs η_{CN_1} under different distances along *z*-axial direction for each hop.

We use d_0 to represent the distance between two adjacent nodes along *z*-axial direction. Then consider three-hop CMC system with two cooperation nodes CN_1 and CN_2, the transmission distance is $3d_0$. **Fig. 6** gives the result the average BEP is changing with detection thresholds when d_0 takes different values. The change trend of average BEP is similar as in Fig. 5. When d_0 is with larger value which results in lower receiving probability, the average BEP is larger and the detection thresholds at lowest point of average BEP are smaller. When d_0=5μm, the average BEP is 0.386 which is larger than that when d_0=3μm, and the corresponding values of detection thresholds at lowest point of BEP are η_{CN_1}=3300, η_{CN_2} =3707, η_D=3721 which are smaller than those when d_0=3μm.

In order to show the differences between DF relay strategy and amplify-and-forward (AF) relay strategy, we give the comparison results in **Fig. 7**. The parameters are set the same for the two relay strategies. Especially, for the AF relay strategy, the amplification factor is set as 5. According to **Fig. 7**, we can see that the average BEP under DF relay strategy decreases faster and is smaller than that under AF relay strategy for the same value of η_{CN_1}. In particular, the detection thresholds at lowest point are the same for these two relay strategies. Therefore, for the CMC system, we choose DF relay strategy.

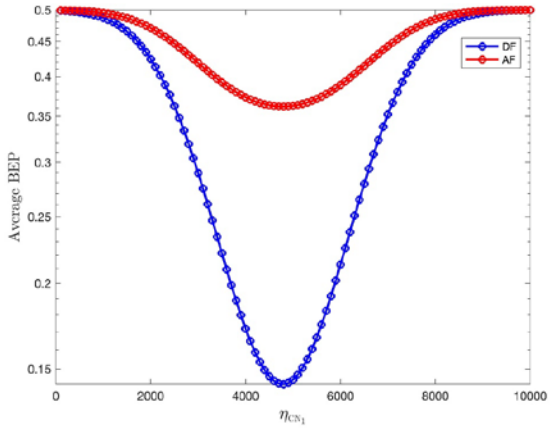

Fig. 7. The average BEP vs η_{CN_1} with DF and AF relay strategies.

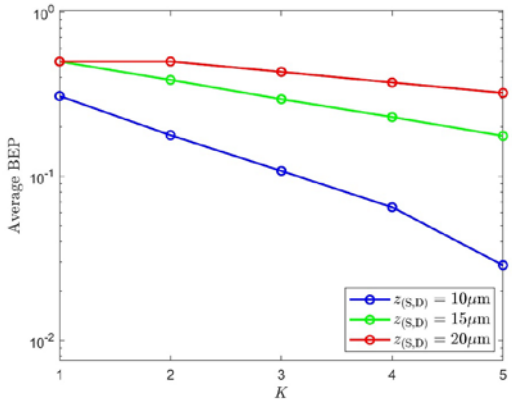

Fig. 8. The average BEP versus *K* under different distances between nodes S and D along *z*-axial direction.

$z_{(S,D)}$ is used to represent the distance between nodes S and D along *z*-axial direction. In **Fig. 8**, the average BEP is decreasing with the value of *K* which is the number of cooperative nodes. When the total distance along *z*-axial direction $z_{(S,D)}$ is fixed, the distance along *z*-axial direction for each hop is decreasing with increasing value of *K*. The receiving probabilities at each cooperative nodes CN_1, CN_2 and node D also increase. Finally, the average BEP is decreasing. For each same value of *K*, the average BEP of this CMC system under $z_{(S,D)}$ =20μm is the lowest than those under $z_{(S,D)}$ =10μm and $z_{(S,D)}$ =15μm.

6. Conclusion

This paper studied the optimizations of multi-hop CMC system in cylindrical anomalous-diffusive channel in a 3D environment. We have derived the average BEP which is optimization objective function. Then the optimization problem for minimizing the average BEP was effectively solved by CG algorithm. The numerical results have shown that CG algorithm can converge by using fewer iterations in contrast to GD algorithm and Bisection algorithm. In addition, we also have shown that some main parameters have impacts on the optimization results. The lager value of α, smaller value of ρ_{cy} and initial distance between two adjacent nodes along *z*-axial direction, then the smaller value of average BEP. In future work, we intend to explore other traditional and efficient optimzaiton methods for solving the optimization problem under the scenario with mobile nodes in CMC system. In additon, we plan to use data driven methods, such as the deep learning methods to optimize optimal detection thresholds under different system parameters for CMC system.

References

[1] I. Llatser, A. Cabellos-Aparicio, and E. Alarcon, “Networking challenges and principles in diffusion-based molecular communication,” *IEEE Wireless Commun.*, vol. 19, no. 5, pp. 36-41, Oct. 2012. Article (CrossRef Link)

[2] T. Nakano, A. Eckford, and T. Haraguchi, *Molecular communication*, New York, NY, USA: Cambridge University Press, 2013. Article (CrossRef Link)

[3] N. Farsad, H. B. Yilmaz, A. Eckford, C. Chae and W. Guo, "A comprehensive survey of recent advancements in molecular communication," *IEEE Commun. Surv. Tutor.*, vol. 18, no. 3, pp. 1887-1919, thirdquarter 2016. Article (CrossRef Link)
[4] T. Nakano, M. J. Moore, F. Wei, A. V. Vasilakos and J. Shuai, "Molecular communication and networking: opportunities and challenges," *IEEE Trans. Nanobioscience*, vol. 11, no. 2, pp. 135-148, Jun. 2012. Article (CrossRef Link)
[5] J. W. Yoo, D. J. Irvine, D. E. Discher, and S. Mitragotri, "Bio-inspired, bioengineered and biomimetic drug delivery carriers," *Nat. Rev. Drug Discov.*, vol. 10, pp. 521-535, Oct. 2011. Article (CrossRef Link)
[6] M. Pierobon and I. F. Akyildiz, "A statistical-physical model of interference in diffusion-based molecular nanonetworks," *IEEE Trans. Commun.*, vol. 62, no. 6, pp. 2085-2095, Jun. 2014. Article (CrossRef Link)
[7] D. Kilinc and O. B. Akan, "Receiver design for molecular communication," *IEEE J. Sel.*, vol. 31, no. 12, pp. 705-714, Dec. 2013. Article (CrossRef Link)
[8] R. L. Fournier, *Basictransport phenomena in biomedical engineering*, Boca Raton, FL, USA: CRC Press, 2017. Article (CrossRef Link)
[9] M. Zoofaghari and H. Arjmandi, "Diffusive molecular communication in biological cylindrical environment," *IEEE Trans. Nanobioscience*, vol. 18, no. 1, pp.74-83, Jan. 2019. Article (CrossRef Link)
[10] H. Arjmandi, M. Zoofaghari, S. V. Rouzegar, M. Veleti´c, and I. Balasingham, "On mathematical analysis of active drug transport coupled with flow-induced diffusion in blood vessels," *IEEE Trans. Nanobioscience*, vol. 20, no. 1, pp. 105-115, Jan. 2021. Article (CrossRef Link)
[11] Y. Lo, C. H. Lee, P. C. Chou, and P. C. Yeh, "Modeling molecular communications in tubes with Poiseuille flow and robin boundary condition," *IEEE Commun. Lett.*, vol. 23, no. 8, pp. 1314-1318, Aug. 2019. Article (CrossRef Link)
[12] S. Dhok, L. Chouhan, A. Noel, and P. K. Sharmay, "Cooperative molecular communication in drift-induced diffusive cylindrical channel," *IEEE Trans. Mol. Biol. Multi Scale Commun.*, vol. 8, no. 1, pp. 44-55, Mar. 2022. Article (CrossRef Link)
[13] T. C. Mai, M. Egan, T. Q. Duong, and M. D. Renzo, "Event detection in molecular communication networks with anomalous diffusion," *IEEE Commun. Lett.*, vol. 21, no. 6, pp. 1249-1252, Jun. 2017. Article (CrossRef Link)
[14] D. P. Trinh, Y. Jeong, H. Shin, and M. Z. Win, "Molecular communication with anomalous diffusion in stochastic nanonetworks," *IEEE Trans. Commun.*, vol. 67, no. 12, pp. 8378-8393, Dec. 2019. Article (CrossRef Link)
[15] L. Chouhan, P. K. Sharma, and A. Noel, "Molecular communication in fractional diffusive channel," *IEEE Commun. Lett.*, vol. 24, no. 10, pp. 2172-2176, Oct. 2020. Article (CrossRef Link)
[16] D. P. Trinh, Y. Jeong, and S. H. Kim, "Molecular communication with passive receivers in anomalous diffusion channels," *IEEE Wireless Commun. Lett.*, vol. 10, no. 10, pp. 2215-2219, Oct. 2021. Article (CrossRef Link)
[17] L. Chouhan, P. K. Upadhyay, P. K. Sharma, and A. M. Salhab, "On anomalous diffusion of devices in molecular communication systems," *IEEE Trans. Mol. Biol. Multi Scale Commun.*, vol. 8, no. 3, pp. 207-211, Jun. 2022. Article (CrossRef Link)
[18] Sh. Dhok, P. Peshwe, P. K. Sharmay, "Cognitive molecular communication in cylindrical anomalous-diffusive channel," *IEEE Trans. Mol. Biol. Multi Scale Commun.*, vol. 8, no. 3, pp. 158-168, Sep. 2022. Article (CrossRef Link)
[19] N. Tavakkoli, P. Azmi, and N. Mokari, "Performance evaluation and optimal detection of relay-assisted diffusion-based molecular communication with drift," *IEEE Trans. Nanobiosci.*, vol. 16, no. 1, pp. 34-42, Jan. 2017. Article (CrossRef Link)
[20] L. Chouhan, P. K. Sharma, and N. Varshney, "On gradient descent optimization in diffusion-advection based 3-D molecular cooperative communication," *IEEE Trans. Nanobiosci.*, vol. 19, no. 3, pp. 347-356, Jul. 2020. Article (CrossRef Link)

[21] Z. Cheng, J. Yan, J. Sun, Y. Tu, and K. Chi, "Joint optimizations of relays locations and decision threshold for multi-hop diffusive mobile molecular communication with drift," *IEEE Trans. Nanobiosci.*, vol. 21, no. 3, 454-465, Jul. 2022. Article (CrossRef Link)
[22] Z. Cheng, Y. Tu, K. Chi, M. Xia. "Optimization of decision thresholds in two-way molecular communication via diffusion with network coding," *IEEE Trans. Mol. Biol. Multi Scale Commun.*, vol. 8, no. 4, pp. 249-262, Jun. 2022. Article (CrossRef Link)
[23] A. Noel, K.C. Cheung, and R. Schober, "Improving receiver performance of diffusive molecular communication with enzymes," *IEEE Trans. Nanobiosci.*, vol. 13, no. 1, pp. 31-43, Jan. 2014. Article (CrossRef Link)
[24] L. Lin, J. Zhang, M. Ma, H. Yan, "Time synchronization for molecular communication with drift," *IEEE Commun. Lett.*, vol. 21, no. 3, 476-479, 2017. Article (CrossRef Link)
[25] V. Jamali, A. Ahmadzadeh, R. Schober, "Symbol synchronization for diffusion-based molecular communications," *IEEE Trans. Nanobiosci.*, vol. 16, no. 8, pp. 873-887, Dec. 2017. Article (CrossRef Link)
[26] L. Chouhan, P. K. Sharma, and A. Noel, "Molecular communication in fractional diffusive channel," *IEEE Commun. Lett.*, vol. 24, no. 10, pp. 2172-2176, Oct. 2020. Article (CrossRef Link)

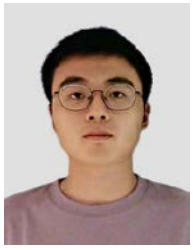

Xuancheng Jin is pursuing the Bachelor's degree in the School of Computer Science and Technology, Zhejiang University of Technology, Hangzhou, China. His research interests include molecular communication and nanonetworks.

Zhen Cheng received the Ph.D. degree in system engineering from Huazhong University of Science and Technology, China, in 2010. She is currently an Associate Professor with the School of Computer Science and Technology, Zhejiang University of Technology, Hangzhou, China. She has published over 40 technical papers in international proceedings and journals. Her current research interests include molecular communication and nanonetworks.

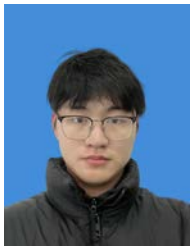

Zhian Ye is pursuing the Bachelor's degree in the School of Computer Science and Technology, Zhejiang University of Technology, Hangzhou, China. His research interests include molecular communication and nanonetworks.

Weihua Gong received the Ph.D. degree in computer software and theory from Huazhong University of Science and Technology, Wuhan, China, in 2006. He is currently an associate professor in School of Computer Science and Technology, Zhejiang University of Technology, China. His research area includes data mining, social networks, and machine learning.